JACS
JOURNAL OF THE AMERICAN CHEMICAL SOCIETY
Article
pubs.acs.org/JACS

Influence of 4′-*O*-Glycoside Constitution and Configuration on Ribosomal Selectivity of Paromomycin

Takahiko Matsushita,[†] Weiwei Chen,[†] Reda Juskeviciene,[‡] Youjin Teo,[‡] Dimitri Shcherbakov,[‡] Andrea Vasella,*[,§] Erik C. Böttger,*[,‡] and David Crich*[,†]

[†]Department of Chemistry, Wayne State University, Detroit, Michigan 48202, United States
[‡]Institut für Medizinische Mikrobiologie, Universität Zürich, 8006 Zürich, Switzerland
[§]Laboratorium für Organische Chemie, ETH Zürich, 8093 Zürich, Switzerland

Supporting Information

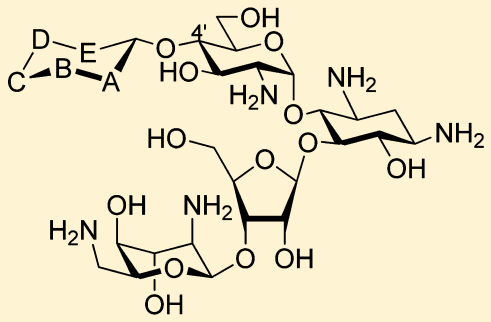

Optimal Design Features for Selectivity

A: O in ring
B: CH_2 preferred, CH-CH_2OH strongly disfavored
C: equatorial OH preferred
D: equatorial OH preferred
E: equatorial OH preferred over axial OH and CH_2

ABSTRACT: A series of 20 4′-*O*-glycosides of the aminoglycoside antibiotic paromomycin were synthesized and evaluated for their ability to inhibit protein synthesis by bacterial, mitochondrial and cytosolic ribosomes. Target selectivity, i.e., inhibition of the bacterial ribosome over eukaryotic mitochondrial and cytosolic ribosomes, which is predictive of antibacterial activity with reduced ototoxicity and systemic toxicity, was greater for the equatorial than for the axial pyranosides, and greater for the D-pentopyranosides than for the L-pentopyranosides and D-hexopyranosides. In particular, 4′-*O*-*β*-D-xylopyranosyl paromomycin shows antibacterioribosomal activity comparable to that of paromomycin, but is significantly more selective showing considerably reduced affinity for the cytosolic ribosome and for the A1555G mutant mitochondrial ribosome associated with hypersusceptibility to drug-induced ototoxicity. Compound antibacterioribosomal activity correlates with antibacterial activity, and the ribosomally more active compounds show activity against *Escherichia coli*, *Klebsiella pneumonia*, *Enterobacter cloacae*, *Acinetobacter baumannii*, and methicillin-resistant *Staphylococcus aureus* (MRSA). The paromomycin glycosides retain activity against clinical strains of MRSA that are resistant to paromomycin, which is demonstrated to be a consequence of 4′-*O*-glycosylation blocking the action of 4′-aminoglycoside nucleotidyl transferases by the use of recombinant *E. coli* carrying the specific resistance determinant.

INTRODUCTION

The continued spread of antibiotic resistant infectious diseases and the meagre pipeline of emerging new drugs to combat them pose a grave threat to the health and economy of modern society.[1−5] Natural product optimization,[6−13] and modification of existing antibacterial drugs hold great promise for antibacterial drug development when informed by knowledge on the mechanisms of action and of resistance. Among antibacterial drugs, the aminoglycoside antibiotics (AGAs)[14−18] are strong candidates for modification and optimization for multiple reasons.[19−21] First, the AGAs continue to be of critical importance for the treatment of methicillin-resistant *Staphylococcus aureus* (MRSA), Gram-negative pathogens, multidrug-resistant *Mycobacterium tuberculosis*, and complex infectious diseases including exacerbated cystic fibrosis, complicated urinary tract infections, sepsis, and chronic obstructive pulmonary disease.[22−24] Second, the mechanism of AGA antibacterial action is known and provides a strong basis for rational optimization.[25−34] Third, existing mechanisms of AGA resistance are well-understood and can be circumvented by design.[35−39] Finally, while much room exists for innovation and improvement, AGA chemistry[40−43] is well developed and enables synthetic planning without undue speculation. Indeed, Plazomicin,[44] a semisynthetic 4,6-disubstituted deoxystreptamine (4,6-DOS)-type of AGA currently in late-stage clinical trials,[16,45] was designed with the above factors in mind. Other modifications of AGAs resulting in higher activity and/or overcoming resistance conferred by members of the aminoglycoside modifying enzyme (AME) family continue to be reported.[46,47]

Received: March 2, 2015
Published: May 29, 2015

ACS Publications © 2015 American Chemical Society

DOI: 10.1021/jacs.5b02248
J. Am. Chem. Soc. 2015, 137, 7706−7717

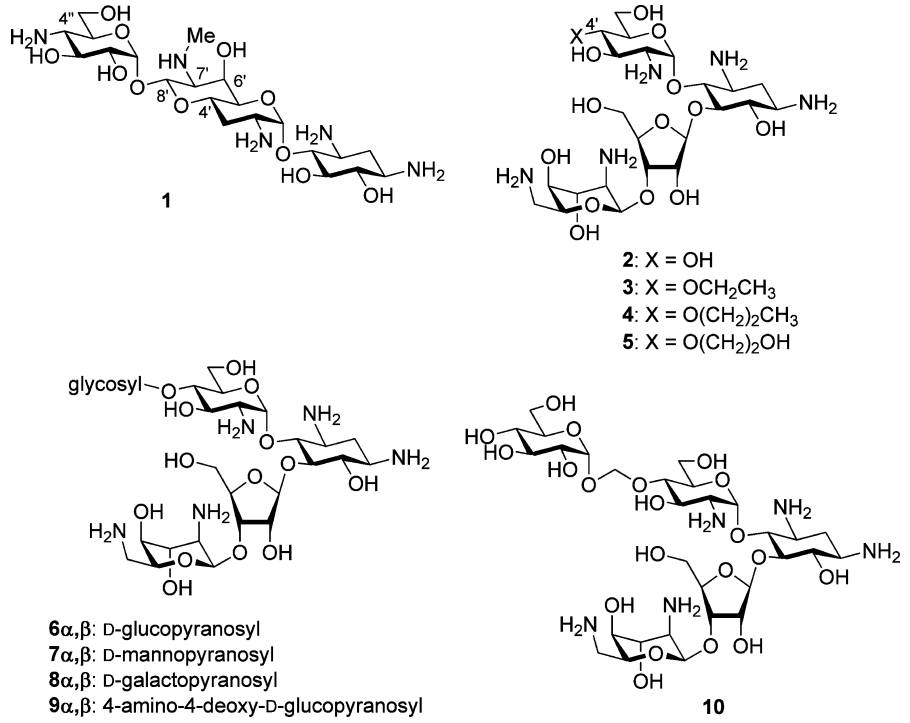

Figure 1. Structures of apramycin, paromomycin, and paromomycin derivatives **3**−**10**.

In addition to being vulnerable to AMEs and other mechanisms of resistance, the AGAs also suffer to varying extents from unwanted side effects such as nephrotoxicity and ototoxicity.[16,18] As AGA uptake by the kidneys is saturable, current clinical regimes minimize nephrotoxicity by the administration of a single large daily dose rather than by continuous infusion. Relatively high doses can thus be administered with a beneficial effect on antibacterial efficacy, while limiting the uptake by the kidneys to the extent that nephrotoxicity is reversible.[48,49] AGA ototoxicity, however, is not reversible, but permanent. It is reported to affect as much as 20% of the patient population,[50,51] with estimates as high as 40% in patients with mycobacterial diseases taking AGAs for long durations.[50,51] Ototoxicity occurs both in a sporadic dose-dependent manner in the general patient population and in an aggravated form in genetically susceptible individuals, with the latter linked to mutations in mitochondrial rRNA, in particular the transition mutation A1555G in the A-site of the mitoribosomal small subunit.[52] Compelling evidence points to a disruption of mitochondrial protein synthesis as a key element in AGA ototoxicity for both sporadic dose-dependent deafness and A1555G-linked mitochondrial hypersusceptibility to AGAs.[53−55] This understanding arises from the ability developed in one of our laboratories to engineer the AGA binding site from eukaryotic rRNA into bacterial 16S rRNA giving rise to bacterial hybrid ribosomes with fully functional eukaryotic rRNA decoding sites, for which cell-free translation assays were developed.[56] While it has also been suggested that AGA binding to human cytoplasmic rRNA contributes to ototoxicity[57] more recent evidence demonstrates that AGA modifications to reduce binding to mitoribosomes while maintaining inhibition of cytoplasmic ribosomes results in lowered ototoxicity in animal models.[58] The evidence for a role of mitochondria in hearing loss in general and in AGA-induced hearing loss in particular is substantial, and has recently been comprehensively reviewed.[53,59−61]

The ability to screen AGAs and their derivatives with cell-free translation assays enables the prediction of the ototoxic potential of a particular compound, whether it arises from AGA inhibition of mitochondrial or cytoplasmic rRNA function. In this manner, the unprecedented dissociation of antibacterial and antimitoribosomal activities in the unusual bicyclic broad spectrum[62,63] AGA, apramycin **1**, has recently been demonstrated with subsequent confirmation of the low ototoxic potential in guinea pigs.[62] We have subsequently demonstrated that modification of the clinically important 4,5-DOS-type AGA paromomycin **2** at the 4′-position yields substances exemplified by **3**-**5** (Figure 1) with greatly increased target selectivity that are essentially devoid of antimitoribosomal and anticytoplasmic ribosomal activity yet retain good antibiotic activity against a spectrum of clinical isolates.[64,65] Two of these substances **3** and **4** were tested in animals and found to be essentially devoid of ototoxicity.[64,65]

In an attempt to improve the activity of the 4′-*O*-alkyl paromomycin derivatives, and building on the structural parallel of apramycin and the 4′-*O*-alkyl paromomycins and on their common binding mode to the decoding A site of the bacterial ribosome,[62,64,66] we synthesized a series of 4′-*O*-D-hexopyranosyl paromomycin derivatives ***6α,β*−*9α,β*** and the 4′-*O*-D-hexopyranosyloxymethyl derivative **10** (Figure 1) and described their antiribosomal and antibacterial activities.[67] In this Article, we complement our earlier work on the paromomycin glycosides through the synthesis and evaluation of a series of 4′-*O*-D- and L-pentopyranosyl paromomycin *α*- and *β*-glycosides and of several 4′-*O*-*α*,*β*-D-pentofuranosyl paromomycin derivatives. We analyze the contributions of substituents around the additional glycosyl ring to antiribosomal selectivity and activity. We show that the activity and especially the ribosomal selectivity of these paromomycin glycosides is configuration dependent and we construct a model and a rationale for their selectivity to guide future work on the synthesis of less toxic and more active AGAs.

DOI: 10.1021/jacs.5b02248
J. Am. Chem. Soc. 2015, 137, 7706−7717

Scheme 1. Synthesis of Glycosides 11−18

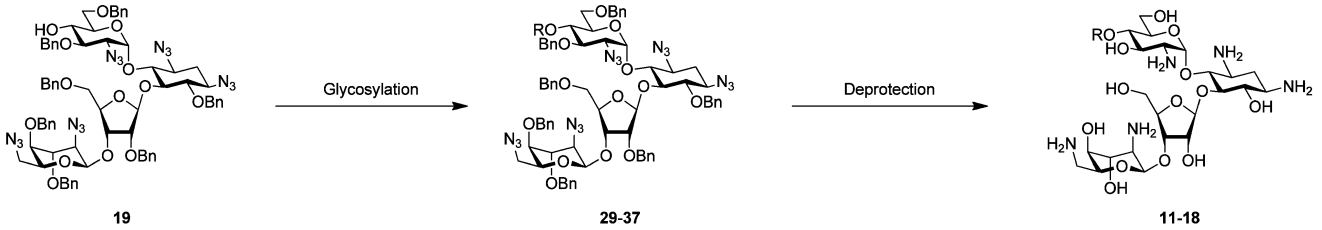

Glycosyl donor	R =				
D-Xylopyranoside	20	29α	29β	11α	11β
L-Xylopyranoside	21	30α	30β	12α	12β
D-Arabinopyranoside	22	31α	31β	13α	13β
L-Arabinopyranoside	23	32α	32β	14α	14β
D-Ribopyranoside	24		33		15β
2-Deoxy-D-xylopyranoside	25		34		16β
D-Arabinofuranoside	26	35		17α	17β
D-Ribofuranoside	27 / 28	36	37	18α	18β

RESULTS

Synthesis. Glycosides **11**−**18** were prepared by glycosylation of the selectively protected paromomycin derivative **19**[67,68] with donors **20**−**28**, followed by deprotection of the immediate glycosylation products **29**−**37**, as summarized in Scheme 1 and in Table 1. Thioglycosides **20**,[69] **22**,[70] **23**,[71] **26**,[72] and **27**[73] were accessed by the literature methods, while thioglycoside **21** was prepared analogously to its enantiomer **20**. Similarly, the trichloroacetimidates **24**[74] and **28**[75] were obtained according to the literature methods or by minor modifications thereof. The 2-deoxy-D-xylopyranose derivative **25** was obtained in 66% yield from 3,4-di-*O*-benzyl-D-xylal[76] according to the method of Fattorusso and co-workers[77] by reaction with *N*-iodosuccinimide (NIS), followed by sodium thiosulfate (see Supporting Information).

For the coupling reactions, the thioglycosides were activated with either diphenyl sulfoxide and trifluoromethanesulfonic anhydride[78] in the presence of tri-*tert*-butylpyrimidine,[79] or with the NIS/trifluoromethanesulfonic acid combination.[80,81] Trichloroacetimidates were activated with either boron trifluoride etherate or trifluoromethanesulfonic acid.[82] Finally, the 2-deoxy-D-xylopyranose derivative **25** was converted into the corresponding α-xylopyranosyl tosylate, which was coupled to the acceptor **19** under the conditions recently described by Bennett for the synthesis of 2-deoxy-β-glycopyranosides.[83,84] All couplings gave anomeric mixtures, with the ratios and yields reported in Table 1, with no attempt made to optimize anomeric selectivity. Deprotection was achieved by Staudinger reduction of the azide groups with trimethylphosphine, followed by hydrogenolysis (Scheme 1 and Table 1). Acetyl protected glycosides were deacetylated according to Zemplén prior to the Staudinger reaction (Scheme 1 and Table 1).

Antiribosomal Activity and Antibacterial Activity. The antiribosomal activities of the glycosylated AGAs against wild-type bacterial ribosomes (Bacterial) and recombinant hybrid ribosomes incorporating the complete A site cassette from human mitochondrial rRNA (Mit13), from the A1555G deafness rRNA allele (A1555G), and from human cytosolic rRNA (Cyt14) were determined in cell-free translation assays. For the purpose of presentation and discussion of the antiribosomal activities obtained in this manner, the data together with those for the previous D-hexopyranosides **6**−**8**[67]

DOI: 10.1021/jacs.5b02248
J. Am. Chem. Soc. 2015, 137, 7706−7717

Table 1. Glycoside Synthesis

	glycosylation			deprotection		
entry	donor (method[a])	product	% yield (α/β)	conditions[f]	product	% yield[g]
1	**20** (A)	**29α**	30	b	**11α**	73
		29β	14	b	**11β**	53
2	**21** (A)	**30α**	22	b	**12α**	63
		30β	32	b	**12β**	32
3	**22** (A)	**31α**	40	b	**13α**	51
		31β	25	b	**13β**	34
4	**23** (A)	**32α**	19	b	**14α**	43
		32β	23	b	**14β**	63
5	**24**[b] (C)	**33**	83[c]	a,b,c	**15β**	25
6	**25** (D)	**34**	10[d]	b	**16β**	61
7	**26** (B)	**35**	42 (2.4)[e]	b,c	**17α**	30
				b,c	**17β**	12
8	**27** (B)	**36**	42 (6.7)[e]	b,c	**18α**	53
9	**28** (C)	**37**	58	a,b	**18β**	50

[a]Glycosylation methods: (A) donor (1.3 equiv), Ph_2SO (1.5 equiv), TTBP (2.9 equiv), Tf_2O (1.5 equiv), CH_2Cl_2, −72 °C, 2 h; (B) donor (1.1 equiv), NIS (1.3 equiv), TfOH (0.1 equiv), CH_2Cl_2, −30 °C, 4 h; (C) donor (2.4 equiv), $BF_3{\cdot}Et_2O$ (1.2 equiv), CH_2Cl_2, −30 °C, 3 h (entry 5), 2 h (entry 9); (D) donor (1.5 equiv), TTBP (1.5 equiv), KHMDS (2.5 equiv), Ts_2O (1.5 equiv), THF, −78 °C, 3 h, then rt, 15 h. [b]Mixture with the corresponding furanoside (pyranoside/furanoside = 1.6). [c]Contained the corresponding furanoside (pyranoside/furanoside = 5.0). The mixture was directly subjected to deprotection without isolation of the pyranoside. [d]Isolated yield from anomeric mixture (78%, α/β = 0.3). [e]The anomeric mixture was directly subjected to deprotection without isolation of one anomer. [f]Deprotection conditions: (a) NaOMe, MeOH, rt; (b) PMe_3, NaOH, THF water, 50 °C, then H_2, $Pd(OH)_2/C$, water, MeOH, AcOH, rt; (c) imidazole-1-sulfonyl azide, K_2CO_3, $CuSO_4$, water/MeOH (1:1), purified by reversed-phase HPLC, then PMe_3, NaOH, THF, water. [g]Overall yield in deprotection.

are presented in the form of two Tables, one (Table 2) for the entire set of equatorial pyranosides and the two β-D-furanosides, and the second (Table 3) for the axial pyranosides and the α-D-furanosides. In both Tables 1 and 2 the glycosides are listed in decreasing order of inhibition of the bacterial ribosome. The activities of paromomycin **2** and its simple acyclic alkyl and hydroxyl alkyl derivatives **3**−**5** are reproduced[65] in Table 4, entries 2−5, for ease of comparison. The Rosanoff nomenclature convention for the anomeric configuration is applied throughout this Article, consequently examples of both α- and β-anomers are found in Tables 2 and 3.[85] The selectivity of the synthetic compounds and of the comparators calculated as the eukaryotic/bacterial activity ratio, is also given in Tables 2−4 for ease of comparison. However, it is stressed that the assumption of a linear relationship between in vitro antiribosomal selectivities and in vivo selectivity is an oversimplification as it neglects possible differences in transport between the different cell types. For example, drug transport into eukaryotic cells is transport-limited, but transport into bacteria is not.[53]

With the view to assessing the general antibacterial activity of these compounds as compared to the parent paromomycin, all compounds were screened for antimicrobial activity. Minimum inhibitory concentrations were determined for clinical isolates of a Gram-positive bacterium (methicillin-resistant *Staphylococcus aureus*, MRSA) and a Gram-negative bacterium (*Escherichia coli*) obtained from the Diagnostic Department of the Institute of Medical Microbiology. All *S. aureus* strains (AG038, AG039, AG042, and AG044) are methicillin-resistant; in addition MRSA strains AG042 and AG044 are resistant to gentamicin. The antimicrobial (MRSA, *E. coli*) data for compounds **11**−**18**, together with those for the earlier hexopyranosides **6**−**8**, and those for the comparators **1**−**5** are presented in Table 5. Additionally, for the more active compounds **11α**, **11β**, **14β**, **18α**, and **15β** and the parent paromomycin **2** minimum inhibitory concentrations (MICs) were determined for clinical isolates of the Gram-negative bacteria *Klebsiella pneumonia*, *Enterobacter cloacae*, *Acinetobacter baumannii*, and *Pseudomonas aeruginosa* (Table 6) obtained from the Diagnostic Department of the Institute of Medical Microbiology. To test the susceptibility of compounds **11α**, **11β**, **14β**, **18α**, and **15β** and the parent paromomycin **2** to common AMEs,[16,35,37,38] MICs were determined for wild-type and recombinant *E. coli* strains carrying defined resistance determinants[62] (Table 7) obtained from Dr. Patrice Courvalin, Institut Pasteur, Paris, France.

DISCUSSION

Glycosylated derivatives of diverse AGAs have been synthesized previously by a number of groups.[86−94] Biological assays, however, have typically been limited to the determination of antibacterial activity and the relatively small numbers of glycosides investigated in any one study have not permitted dissection of the contributions to activity of the substituents around the added carbohydrate ring. Extending our preliminary studies with a series 4′-*O*-D-hexopyranosyl paromomycin derivatives,[67] the 4′-*O*-D- and L-pentopyranosyl and D-pentofuranosyl paromomycin glycosides whose synthesis we report here make available a diverse set of 20 paromomycin 4′-*O*-glycosides with which to construct a structure activity relationship. Inspection of the antibacterioribosomal and antimitoribosomal activity of the 16 available pyranosides suggested a separate consideration of the equatorial and the axial glycosides (Tables 2 and 3), with the axial glycosides exhibiting in particular significantly lower selectivity as a consequence of their greater activity for the recombinant hybrid ribosomes carrying the mitochondrial A site rRNA cassette. The two β-D-furanosides were then added to the ensemble of equatorial pyranosides, and the two α-D-furanosides to the groups of axial pyranosides because of the greater structural parallels; these placements being supported by the antimitoribosomal activities, which are significantly greater for the α-D-furanosides than for their β-epimers (Tables 2 and 3). In Tables 2 and 3 the compounds are sorted in terms of descending antibacterioribosomal activity to facilitate pattern recognition. The pattern noted earlier for the D-hexopyranosides, whereby the axial series were consistently more active than the equatorial series,[67] does not extend to the more extensive data set now presented, as the equatorial β-D-xylopyranoside exhibits the strongest inhibition of the bacterial ribosome among the pyranosides. The allocation of the data into the two series (Tables 2 and 3) for separate consideration not only reflects different antiribosomal activity and selectivity patterns, but is logical in view of the projection of the appended glycosides in different directions from the paromomycin 4′-position. This postulate is subject to the proviso that all the glycosides under study adopt the standard conformations and preferred glycosidic torsion angles,[95−97] as depicted in the structures in Tables 2 and 3. Indeed, analysis[98−102] of the NMR data indicates that all pento- and hexopyranosides predom-

DOI: 10.1021/jacs.5b02248
J. Am. Chem. Soc. 2015, 137, 7706−7717

Table 2. Antiribosomal Activities and Selectivities of the Paromomycin Equatorial Pyranosides and β-D-Furanosides (IC_{50}, μg/mL)

Entry	Compound[a]	Bacterial[b]	Mit13[b] (selectivity)[c]	A1555G[b] (selectivity)[c]	Cyt14[b] (selectivity)[c]
1	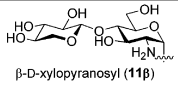 β-D-xylopyranosyl (**11β**)	0.03±0.01	34.51±17.20 (1150)	28.02±14.45 (934)	25.03±9.85 (834)
2	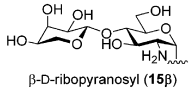 β-D-ribopyranosyl (**15β**)	0.04	11.48 (287)	71.10 (1778)	62.35 (1559)
3	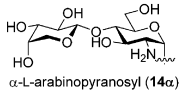 α-L-arabinopyranosyl (**14α**)	0.16	34.57 (216)	64.55 (403)	113.97 (712)
4	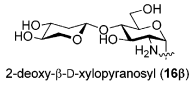 2-deoxy-β-D-xylopyranosyl (**16β**)	0.26	69.77 (268)	66.81 (256)	197.37 (759)
5	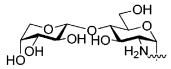 α-D-arabinopyranosyl (**13α**)	0.28	10.87 (39)	21.91 (78)	64.17 (229)
6	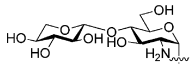 β-L-xylopyranosyl (**12β**)	0.30	20.34 (67.8)	32.84 (109)	45.30 (151)
7	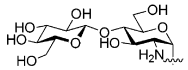 β-D-glucopyranosyl (**6β**)	0.37	59.12 (160)	83.64 (226)	117.53 (318)
8	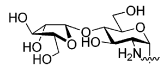 β-D-arabinofuranosyl (**17β**)	0.45	67.51 (150)	102.98 (229)	107.13 (238)
9	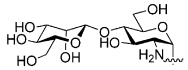 β-D-mannopyranosyl (**7β**)	0.46	54.60 (119)	85.70 (186)	90.35 (196)
10	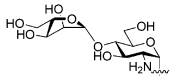 β-D-ribofuranosyl (**18β**)	0.63	65.15 (103)	102.86 (163)	94.93 (151)
11	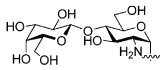 β-D-galactopyranosyl (**8β**)	1.52	141.35 (93)	209.22 (138)	286.76 (189)

[a]The partial structures in the table show the appended glycoside and ring I of paromomycin. [b]With the exception of entry 1, for which activities were determined in triplicate, activities are for single-point determinations using two-fold dilution series. The standard deviations of such measurements are typically ±50% of the measured activity, as is seen from entry 1 and from the comparators (Table 4). [c]Antiribosomal activity/antibacterioribosomal activity.

inantly adopt the chair conformations indicated in Tables 2 and 3. The NMR data for the furanosides suggest that the conformation of the β-D-arabinofuranoside **17β** is best described by a $^{\circ}E \sim {}_1T^{\circ} \sim {}_1E$ equilibrium, and that of its α-anomer **17α** by ${}_4E \sim {}_4T^{\circ} \sim {}^{\circ}E$. The vicinal coupling constants exhibited by the β-D-ribofuranoside **18β** indicate that its preferred conformation is located on the ${}^3E \sim {}^3T_4 \sim {}_4E$ segment of the furanoside pseudorotational itinerary, while the α-anomer **18α** can be considered to populate both the ${}^1E \sim {}_2T^1 \sim {}_2E$ and the $^{\circ}E \sim {}_1T^{\circ} \sim {}_1E$ conformations on the basis of the NMR data available. The assignment of the a $^{\circ}E \sim {}_1T^{\circ} \sim {}_1E$ to the β-D-arabinofuranoside **17β** differs from the NMR analysis of methyl β-D-arabinofuranoside and from a recent statistical analysis[103] of X-ray crystallographic data, all of which cluster the D-arabinofuranosides in the northwestern portion of the pseudorotational wheel around the E_3 conformer. However, among the β-D-arabinofuranosides considered in that analysis, only one[104] had a complex aglycone, with all others being simple methyl β-D-arabinofuranosides lacking the possibility of intramolecular hydrogen bonding to the aglcyone. The conformations assigned to the β-D-ribofuranoside **18β**, the α-D-arabinofuranoside **17α**, and at least for one ($^{\circ}E \sim {}_1T^{\circ} \sim {}_1E$) of the two possible conformations in the α-D-ribofuranoside **18α** are consistent with or close to those reported in the statistical analysis of crystallographic data.[103] In Tables 2 and 3, a single one of the possible conformations of the arabino- and

DOI: 10.1021/jacs.5b02248
J. Am. Chem. Soc. 2015, 137, 7706−7717

Table 3. Antiribosomal Activities and Selectivities of the Paromomycin Axial Pyranosides and the α-D-Furanosides (IC_{50}, μg/mL)

Entry	Compound[a]	Bacterial[b]	Mit13[b] (selectivity)[c]	A1555G[b] (selectivity)[c]	Cyt14[b] (selectivity)[c]
1	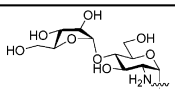 α-D-arabinofuranosyl (**17α**)	0.03	7.88 (263)	30.67 (1022)	56.86 (1895)
2	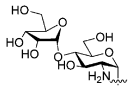 α-D-ribofuranosyl (**18α**)	0.03	6.28 (209)	20.98 (699)	27.26 (909)
3	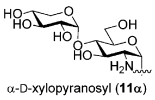 α-D-xylopyranosyl (**11α**)	0.10	3.58 (36)	12.06 (121)	37.42 (374)
4	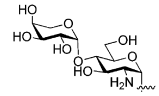 β-L-arabinopyranosyl (**14β**)	0.12	3.51 (29)	11.28 (94)	52.77 (440)
5	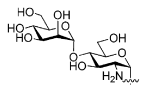 α-D-mannopyranosyl (**7α**)	0.29	2.19 (8)	18.05 (62)	51.72 (178)
6	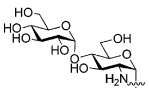 α-D-glucopyranosyl (**6α**)	0.32	1.86 (6)	13.98 (47)	46.26 (145)
7	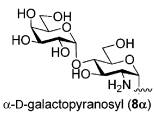 α-D-galactopyranosyl (**8α**)	0.55	2.23 (4)	14.95 (27)	35.63 (65)
8	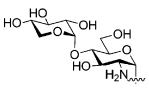 α-L-xylopyranosyl (**12α**)	0.61	7.01 (11.5)	31.95 (52.4)	78.94 (129)
9	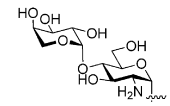 β-D-arabinopyranosyl (**13β**)	0.67	3.73 (5.6)	25.68 (38)	74.63 (111)

[a]The partial structures in the table show the appended glycoside and ring I of paromomycin. [b]Activities are for single-point determinations using two-fold dilution series. The standard deviations of such measurements are typically ±50% of the measured activity, as is seen from the comparators (Table 4). [c]Antiribosomal activity/antibacterioribosomal activity.

Table 4. Antiribosomal Activities and Selectivities of the Comparators 1−5 (IC_{50}, μg/mL)

entry	cmpd	Bacterial[a]	Mit13[a] (selectivity)[b]	A1555G[a] (selectivity)[b]	Cyt14[a] (selectivity)[b]
1	apramycin (**1**)	0.06 ± 0.03	58.03 ± 18.80 (967)	26.06 ± 7.08 (434)	49.17 ± 11.95 (819)
2	paromomycin (**2**)	0.02 ± 0.01	50.19 ± 11.84 (2510)	5.39 ± 2.05 (270)	9.41 ± 2.68 (471)
3	4′-*O*-ethyl paromomycin (**3**)	0.08 ± 0.03	99.27 ± 12.51 (1240)	114.73 ± 34.07 (1434)	102.90 ± 31.34 (1286)
4	4′-*O*-propyl paromomycin (**4**)	0.10 ± 0.02	103.79 ± 6.50 (1038)	75.74 ± 8.50 (757)	83.84 ± 14.52 (834)
5	4′-*O*-(2-hydroxyethyl) paromomycin (**5**)	0.05 ± 0.02	87.49 ± 22.29 (1750)	81.35 ± 14.81 (1627)	74.36 ± 10.08 (1487)

[a]Mean ± standard deviation of three measurements. [b]Antiribosomal activity/antibacterioribosomal activity.

ribofuranosides is represented; a more complete rendering is given in the Supporting Information.

Consideration of the antiribosomal activities of the nine equatorial pyranosides (Table 2) leads to a set of generalizations on the effect of substitution at the various positions around the appended glycosidic ring (Figure 2). The four compounds most active against the bacterial ribosome (Table 2, entries 1−4) all have an oxygen atom in the ring at position A and a methylene group at position B. The preferential location of a ring oxygen at position A may reflect hydrogen bonding to the ribosome or to the proximal 3′-hydroxy group of the paromomycin ring I. The latter, which is analogous to the

DOI: 10.1021/jacs.5b02248
J. Am. Chem. Soc. 2015, 137, 7706−7717

Table 5. Antimicrobial Data against MRSA and *E. coli* for Paromomycin 4′-*O*-Glycosides and for Comparators 1−5 (MIC, μg/mL)[a]

	MRSA				*E. coli*		
strain:	AG038	AG039	AG042	AG044	AG001	AG055	AG003
apramycin (**1**)	8	8	8	8−16	16	8	8−16
paromomycin (**2**)	4	>256	>256	4−8	16−32	8	8−16
4′-*O*-ethyl paromomycin (**3**)	8−16	16	8−16	8−16	32−64	32−64	32
4′-*O*-propyl paromomycin (**4**)	8−16	16	8−16	8	32	32	32
4′-*O*-(2-hydroxy-ethyl) paromomycin (**5**)	32	32	16−32	32−64	32−64	32−64	32
α-D-xylopyranosyl paromomycin (**11α**)	8	16	8	8	32	32	32
β-D-xylopyranosyl paromomycin (**11β**)	16	16	8−16	16	16	16	16
β-L-arabinopyranosyl paromomycin (**14β**)	16	16	16	16	64	32	32−64
β-D-ribopyranosyl paromomycin (**15β**)	16−32	32	16	32	32	16−32	16−32
α-D-arabinofuranosyl paromomycin (**17α**)	32	32	32	32	64	64	32−64
α-D-Ribofuranosyl paromomycin (**18α**)	32	32	16−32	16−32	32	32	32
α-L-arabinopyranosyl paromomycin (**14α**)	32	32	32	32	>64	>64	>64
α-D-glucopyranosyl paromomycin (**6α**)	32	32	32	16−32	128	128	128
β-L-xylopyranosyl paromomycin (**12β**)	32−64	≥64	32−64	32−64	>64	>64	>64
α-D-galactopyranosyl paromomycin (**8α**)	64	128	64	64	>128	>128	>128
α-D-mannopyranosyl paromomycin (**7α**)	64	≥128	>128	32−64	>128	>128	≥128
α-D-arabinopyranosyl paromomycin (**13α**)	64	≥64	32−64	64	>64	>64	>64
β-D-arabinopyranosyl paromomycin (**13β**)	>64	>64	>64	>64	>64	>64	>64
α-L-xylopyranosyl paromomycin (**12α**)	>64	>64	>64	>64	>64	>64	>64
2-deoxy-β-D-xylopyranosyl paromomycin (**16β**)	64	≥128	128	64	128	128	128
β-D-glucopyranosyl paromomycin (**6β**)	128	≥128	>128	128	>128	>128	>128
β-D-galactopyranosyl paromomycin (**8β**)	≥128	≥128	>128	>128	>128	>128	>128
β-D-mannopyranosyl paromomycin (**7β**)	≥128	≥128	≥128	≥128	>128	>128	>128
β-D-arabinofuranosyl paromomycin (**17β**)	≥128	≥128	128	128	≥128	≥128	≥128
β-D-ribofuranosyl paromomycin (**18β**)	>128	>128	>128	>128	>128	>128	>128

[a]All values were determined in triplicate using two-fold dilution series.

Table 6. Antimicrobial Data against *Pseudomonas aeruginosa*, *Acinetobacter baumannii*, *Enterobacter cloacae*, and *Klebsiella pneumoniae* for Paromomycin and Selected 4′-*O*-Glycosides (MIC, μg/mL)[a]

	P. aeruginosa		*A. baumannii*			*En. cloacae*			*K. pneumoniae*		
strain:	AG031	AG032	AG107	AG108	AG109	AG112	AG113	AG114	AG115	AG116	AG118
paromomycin (**2**)	>128	>128	4	4−8	4	4	4−8	4−8	4	4	8
α-D-xylopyranosyl paromomycin (**11α**)	>128	>128	32	32	16	32	32	32	32	32	32
β-D-xylopyranosyl paromomycin (**11β**)	32−64	32−64	16−32	16−32	16	16−32	16−32	32	16−32	16	32
β-L-arabinopyranosyl paromomycin (**14β**)	32−64	32−64	16	16	8	16−32	16−32	16−32	16−32	16	32
β-D-ribopyranosyl paromomycin (**15β**)	16−32	16−32	16	16	8	16	16	16−32	16	16	16−32
α-D-arabinofuranosyl paromomycin (**17α**)	64−128	64−128	32	32	32	32	32	32	32	32	32
α-D-ribofuranosyl paromomycin (**18α**)	32−64	32−64	32	32	8−16	16	16	16	16	16	16

[a]All values were determined in duplicate using two-fold dilution series.

3-OH−O5′ hydrogen bond found in β-1,4-linked di- and higher saccharides such as cellobiose,[95,105−110] would reduce conformational mobility about the glycosidic bond and thereby enhance the interaction of other ring substituents with the target by lowering any entropic penalty. The three most active compounds (Table 2, entries 1−3) all have an equatorial hydroxyl group at position E, whose removal (Table 2, entry 4) leads to a loss of antibacterioribosomal activity. An equatorial orientation for the hydroxyl groups at positions C and D is preferred (Table 1, entries 1−3), at the former for antibacterioribosomal activity and at the latter for reduced inhibition of the mitochondrial ribosome. Conversely, relocation of the ring oxygen to position E and installation of an equatorial hydroxyl group at position A (Table 2, compare entries 1 with 6, and 3 with 5) reduces activity. The hexopyranosides (Table 2, entries 7, 9, and 11) are routinely less active for bacterial ribosomes than the pentopyranosides (Table 2, entries 1−6) indicating that the inclusion of an equatorial hydroxymethyl group at position B is detrimental for binding, presumably because of a steric clash with the ribosome. The small preference for an equatorial hydroxyl group at position E is seen by comparison of entries 7 and 9 (Table 2), while that for the equatorial hydroxyl group at position C is supported by comparison of entries 1 and 7 with 3 and 11

DOI: 10.1021/jacs.5b02248
J. Am. Chem. Soc. 2015, 137, 7706−7717

Table 7. Antimicrobial Data against Wild-Type and Engineered Strains of *E. coli* Carrying Specific Resistance Determinants for Paromomycin and Selected 4′-*O*-Glycosides (MIC, μg/mL)[a]

	strain					
	BM13 (AG006)	AG007	AG008	AG009	AG036	AG037
resistance mechanism:	–	AAC(3)	ANT(2″)	AAC(6′)	ANT(4′,4″)	APH(3′,5″)
paromomycin (**2**)	2–4	8	4–8	8	>128	>128
α-D-xylopyranosyl paromomycin (**11α**)	16	64	8–16	64	16–32	>128
β-D-xylopyranosyl paromomycin (**11β**)	4–8	16–32	4–8	16	8	>128
β-L-arabinopyranosyl paromomycin (**14β**)	8–16	32	4–8	32	8–16	>128
β-D-ribopyranosyl paromomycin (**15β**)	4–8	16–32	4–8	16	8	>128
α-D-arabinofuranosyl paromomycin (**17α**)	8	32	8	32	8–16	>128
α-D-ribofuranosyl paromomycin (**18α**)	4–8	16–32	4–8	16	8	>128

[a]All values were determined in duplicate using two-fold dilution series.

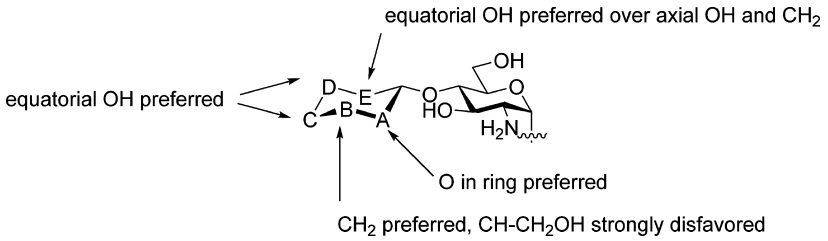

Figure 2. Preferred ring substituents in the equatorial pyranosides.

(Table 2). The two furanosides carry hydroxymethyl groups which will project into approximately the same space as the identical group at position B of the pyranosides and therefore presumably have only modest activity because of a comparable steric clash. Comparison of the equatorial pyranosides with paromomycin (Table 4) reveals that the best equatorial pyranosides **11β** and **15β** (Table 2, entries 1 and 2) have comparable affinity for the bacterial ribosomes and lower affinity for the deafness mitochondrial allele and cytoplasmic ribosome than paromomycin (Table 4, entry 2). Compounds **11β** and **15β** have greater activity for the bacterial ribosome than the optimal 4′-*O*-alkyl paromomycin derivatives 3 and 4 (Table 4, entries 3 and 4) and comparable activity to the 4′-*O*-hydroxyethyl derivative 5 (Table 4, entry 5). Therefore, compounds **11β** and **15β** retain the activity of paromomycin and have selectivity comparable to the 4′-*O*-alkyl paromomycin derivatives, which clearly establishes the possibility of preparing novel highly active AGAs with reduced potential for ototoxicity.

The construction of a model for the axial pyranosides and the two associated α-D-furanosides (Table 3) is both more difficult than for the equatorial pyranosides and ultimately less relevant owing to the routinely greater affinity of this compound series for the mitochondrial ribosome. The proportionately greater activity of this series of compounds (Table 3) against the mitochondrial ribosome results in less selectivity and is predictive of ototoxicity. Consequently the pertinence of this series of compounds is reduced from a drug discovery perspective. It is nevertheless noteworthy that the two furanosides are the compounds most active against bacterial ribosomes (Table 3, entries 1 and 2), that the activity is not dependent on the configuration at the 2-position of the furanoside ring, and that it is comparable to the activity of paromomycin (Table 4, entry 2). As in the equatorial series, passage from an axial pentopyranoside to the hexopyranoside of the same configurational series results in a significant loss of activity (Table 3, compare entries 3 with 6, and 4 with 7). However, as the highly active furanosides **17α** and **18α** both retain a hydroxymethyl group in approximately the same region of space as the hexopyranosides **6α**, **7α**, and **8α** the reduced activity of the latter is likely not due to a steric clash of the hydroxymethyl group with the target. Rather, in the axial series it appears that the more active compounds are the more conformationally mobile ones; furanosides typically having lower barriers to pseudorotation than the conformational inversion of pyranosides, and pentopyranosides undergoing conformational change more readily than hexopyranosides. That the two pentopyranosides **12α** and **13β** (Table 3, entries 8 and 9) are the least active compounds in this series indicates that the location of the ring oxygen in the appended sugar is important. Possibly, a hydrogen bond from the 3′-OH in the paromomycin ring I to this ring oxygen in **12α** and **13β** may have a rigidifying effect on the global conformation of these two saccharides which is disruptive to the interaction with the target. Alternatively, and as found in all other axial pyranosides (Table 3), a hydroxyl group on the front side of the pyranoside ring in the position occupied by the ring oxygen in **12α** and **13β** makes an important contribution to binding.

Overall, a more specific interaction with the decoding A site is indicated for the equatorial pyranosides and the corresponding β-D-furanosides (Table 2) than for the axial pyranosides and the associated α-D-furanosides (Table 3). This postulate is consistent with the reduced selectivity in the latter series, with the changes in the ribosomal RNA (rRNA) decoding A site having less influence on specific interactions with the glycosylated aminoglycoside.

The pattern of antiribosomal activity of the 4′-*O*-glycosyl paromomycin derivatives, and the manner in which these activities depend on the precise base sequence of the decoding A site, strongly suggests that these compounds bind the decoding A site of helix 44 of prokaryotic rRNA in a manner analogous to that established crystallographically for paromomycin,[25] apramycin,[62] and other 4′-*O*-derivatives of paromomycin.[64] In these AGA·rRNA complexes, which are characteristic for all 4,5-series AGAs,[27] the β-face of the AGA ring I

DOI: 10.1021/jacs.5b02248
J. Am. Chem. Soc. 2015, 137, 7706–7717

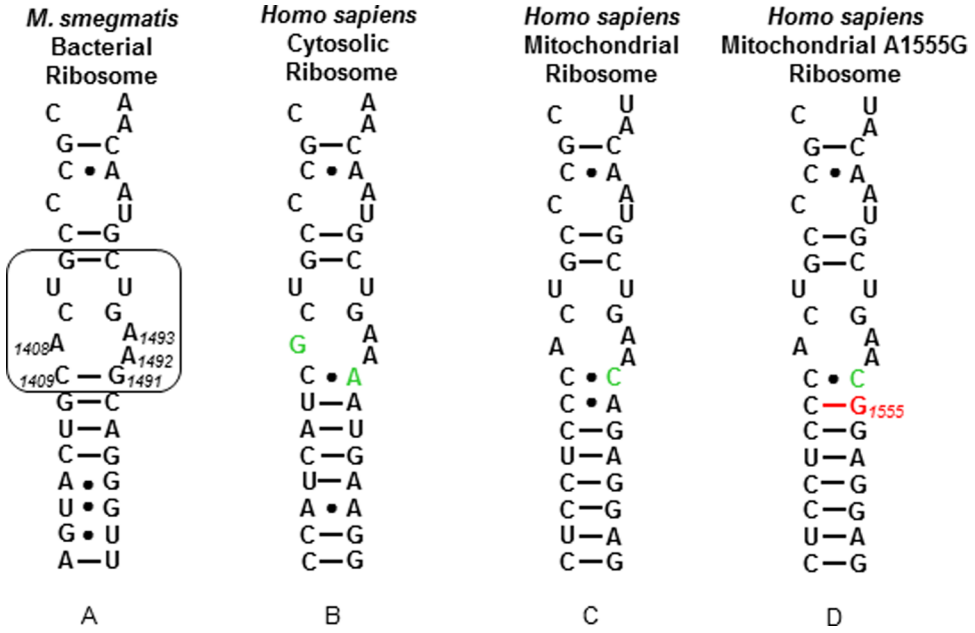

Figure 3. Decoding A sites of prokaryotic and eukaryotic ribosomes. The AGA binding pocket is boxed. The bacterial numbering scheme is illustrated for the AGA binding pocket. Changes from the bacterial ribosome binding pocket are colored green. The A1555G mutant conferring hypersusceptibility to AGA ototoxicity is colored red.

stacks onto G1491 and interacts with it via a 4′-CH–π interaction. In the bound structures the decoding A site has the bases A1492 and A1493 in the flipped out mode that is an integral part of the decoding mechanism.[111] For the crystallographically examined 4′-*O*-benzyl paromomycin and 4′,6′-*O*-benzylidene paromomycins, the 4′-substituent extends into an area of bulk water close to the G1491-3′-OP(O_2^-)-O-5′-A1492 phosphate group;[64] the 4-aminoglucopyranosyl moiety of apramycin occupies the same space in its complex with the decoding A site.[62] Given that the 4′-*O*-glycosyl paromomycin derivatives bind in a standard manner, the glycosyl moiety will necessarily occupy the same hydrated region of the decoding A site backbone in proximity to the phosphate ester spanning G1491 and the flipped out A1492. The systematic variation between the equatorial and axial series of glycosides stems from the occupancy of contiguous but different parts of this binding site.

The origin for the aminoglycosides' selective inhibition of bacterial ribosomes stems from the bases lining the decoding A site (Figure 3).[112] Thus, the decoding A site of the cytoplasmic ribosome (Figure 3B) differs from that of the bacterial ribosome (Figure 3A) by two base substitutions (A1408G and G1491A), both of which affect key interactions with the aminoglycoside ring I. In the mitochondrial ribosome (Figure 3C), the single substitution (G1491C) in the binding site impinges on the CH-π interaction of that base with the β-face of the AGA ring I.[54] The mitochondrial decoding A site is also characterized by the presence of a second non-canonical base pair immediately underneath the floor of the binding site, presumably resulting in greater flexibility and thus contributing to the lower affinity for AGAs. When this second non-canonical base pair is replaced by a Watson–Crick pair, as in the A1555G deafness allele (Figure 3D), affinity for AGA is enhanced and hypersusceptibility to aminoglycoside ototoxicity results.[55] Evidently, the paromomycin 4′-*O*-axial glycopyranosides and the corresponding α-D-furanosides (Table 3) enjoy a more favorable interaction with the mitochondrial decoding A site than the 4′-*O*-equatorial glycopyranosides (Table 2), which leads to the differing selectivity profiles of the two series of compounds. Compared to the parental paromomycin, the series of 4′-*O*-glycosylated derivatives synthesized is less active on A1555G mutant mitoribosomes and cytosolic ribosomes. In general, activity of the compound series for cytosolic Cyt14 ribosomes is in the same range as that for mitoribosomal A1555G mutant hybrid ribosomes. This is similar for paromomycin, but significantly different from aminoglycosides (both 4,5 and 4,6) with a 6′-NH_2 substituent. Apparently, as long as there is no steric clash between ring I and residue 1408 (a 6′-NH_2 results in a steric clash with the cytosolic G1408),[113] the drug binding pockets of cytosolic Cyt14 recombinant ribosomes and mitochondrial deafness A1555G recombinant ribosomes are quite similar at the structural level—1409/1491 C/A vs C/C, base pairing between 1410/1490. Although cryo-electron-microscopy structures of mitochondrial ribosomes have recently appeared and are consistent with the above hypotheses,[114,115] X-ray crystal structures are not yet available for the 4,5-series AGA in complex with the complete cytosolic ribosome or for any AGA bound to a mitochondrial ribosome. Further discussion of the exact nature of the interactions between 4,5-AGAs and the eukaryotic decoding A sites therefore would be overly speculative.

The pattern of antibacterial activity of the 4′-*O*-glycosyl paromomycin derivatives largely follows the antibacterioribosomal activity, especially for the pyranosides. Thus, for example, the β-D-xylopyranosyl derivative **11*β***, with the highest antiribosomal activity (Table 2) shows good antibacterial activity against clinical strains of the Gram-positive MRSA and the Gram-negative *E. coli* (Table 5), comparable in most cases with apramycin, paromomycin, and the 4′-*O*-alkyl paromomycins **3** and **4**. Correspondingly, the least ribosomally active glycosides show the lowest levels of antibacterial activity against MRSA and *E. coli*. The exceptions to this overall pattern are the two α-D-furanosyl derivatives **17*α*** and **18*α*** which display somewhat lower antibacterial activity (Table 5) than would

DOI: 10.1021/jacs.5b02248
J. Am. Chem. Soc. 2015, 137, 7706–7717

have been expected on the basis of antiribosomal activity alone (Table 3). These and other minor differences between antiribosomal and antibacterial activity reflect the change from an in vitro system using a cell-free translation assay to an assay measuring the inhibition of growth of live bacteria with all the associated complications of drug transport and efflux. The overall corresponding pattern of antibacterioribosomal activity (Table 3) and antibacterial activity extends to the clinically important Gram-negative pathogens *A. baumannii*, *En. cloacae*, and *K. pneumonia* (Table 6). In contrast to the parent paromomycin, the 4′-*O*-glycosides in part display notable activity against the Gram-negative bacterium *P. aeruginosa* (Table 6). In addition, the paromomycin 4′-*O*-glycosides retain activity against clinical isolates AG039 and AG042 of MRSA for which paromomycin itself shows no activity (Table 5). This feature is common to apramycin and to the 4′-*O*-alkyl paromomcyins (Table 5), suggesting that derivatization at the 4′-position overcomes the action of a 4′-aminoglycoside modifying enzyme.[116,117] This hypothesis is supported by comparing the activity of the 4′-*O*-glycosides to that of paromomycin against recombinant *E. coli* carrying the 4′,4″-aminoglycoside nucleotidyl transferase (ANT(4′,4″)) resistance determinant (Table 7). As expected 4′-*O*-glycosylation does not suppress the action of 3′-aminoglycoside phosphatases (APH(3′)) or the low level activity of the 3- and 6′-aminoacyl transferases ((AAC3 and AAC6′) (Table 7). These data indicate that future generations of aminoglycosides can be designed to overcome ototoxicity and one or more resistance mechanisms through the use of a single modification.

CONCLUSION

The synthesis of an extensive series of 4′-*O*-glycosylated paromomycin derivatives and their screening for inhibition of protein synthesis in cell-free translation assays using bacterial wild-type and recombinant hybrid ribosomes has revealed patterns that should aid in the design of further improved and more selective aminoglycoside antibiotics. Equatorial glycosides typically bind the mitochondrial ribosome less tightly than their axial anomers and are therefore the anomers of choice in the future development of less ototoxic 4′-*O*-glycosylated aminoglycosides. In both the axial and equatorial series the pentopyranosides, lacking the hydroxymethyl side chain, are more active than the comparable hexopyranosides. Certain isomers of the pentopyranosides, especially the β-D-xylopyranoside, have antibacterioribosomal activity comparable to paromomycin and a selectivity profile that approaches that of apramycin, for which reduced ototoxicity has been demonstrated. The 4′-*O*-glycosylated paromomycin derivatives are not susceptible to modification by ANT(4′,4″) aminoglycoside modifying enzymes leading to the possibility that single synergistic modifications can be designed into future generations of AGAs to reduce toxicity and overcome resistance mechanisms.

ASSOCIATED CONTENT

Supporting Information

Full experimental details and ^{1}H and ^{13}C NMR spectra for all new compounds. The Supporting Information is available free of charge on the ACS Publications website at DOI: 10.1021/jacs.5b02248.

AUTHOR INFORMATION

Corresponding Author

*dcrich@chem.wayne.edu

Notes

The authors declare no competing financial interest.

ACKNOWLEDGMENTS

We thank the University of Zurich and Wayne State University for support of this work, and acknowledge support from the NSF (MRI-084043) for the purchase of the 600 MHz NMR spectrometer in the Lumigen Instrument Center at Wayne State University. We thank P. Courvalin, Institut Pasteur, for recombinant *E. coli* strains.

REFERENCES

(1) Holdren, J. P.; Lander, E. S. *Report to the President on Combatting Antibiotic Resistance*; President's Council of Advisors on Science and Technology , Washington DC, Sept 2014.

(2) Payne, D. J.; Gwynn, M. N.; Holmes, D. J.; Pompliano, D. L. *Nat. Rev.: Drug Discovery* **2007**, *6*, 29−40.

(3) French, G. L. *Int. J. Antimicrob. Agents* **2010**, *36* (Suppl 3), S3−S7.

(4) Walsh, C. T. *Chem. Rev.* **2009**, *105*, 391−744.

(5) Karaiskos, I.; Giamarellou, H. *Exp. Opin. Pharmacother.* **2015**, *15*, 1351−1370.

(6) Wright, P. M.; Seiple, I. B.; Myers, A. G. *Angew. Chem., Int. Ed.* **2014**, *53*, 8840−8863.

(7) Nicolaou, K. C. *Angew. Chem., Int. Ed.* **2014**, *53*, 9128−9140.

(8) Li, J. W.-H.; Vederas, J. C. *Science* **2009**, *325*, 161−165.

(9) Wright, G. D.; Sutherland, A. D. *Trends Mol. Med.* **2007**, *13*, 260−267.

(10) Butler, M. S.; Buss, A. D. *Biochem. Pharmacol.* **2006**, *71*, 919−929.

(11) Walsh, C. T.; Fischbach, M. A. *J. Am. Chem. Soc.* **2010**, *132*, 2469−2493.

(12) Newman, D. J.; Cragg, G. M. *J. Nat. Prod.* **2007**, *70*, 461−477.

(13) Connell, K. M. G. O.; Hodgkinson, J. T.; Sore, H. F.; Welch, M.; Salmond, G. P. C.; Spring, D. R. *Angew. Chem., Int. Ed.* **2013**, *52*, 10706−10733.

(14) *Aminoglycoisde Antibiotics: From Chemical Biology to Drug Discovery*; Arya, D. P., Ed.; Wiley: Hoboken, NJ, 2007.

(15) Haddad, J.; Kotra, L. P.; Mobashery, S. In *Glycochemsitry: Principles, Synthesis, and Applications*; Wang, P. G., Bertozzi, C. R., Eds.; Dekker: New York, 2001; pp 307−351.

(16) Armstrong, E. S.; Kostrub, C. F.; Cass, R. T.; Moser, H. E.; Serio, A. W.; Miller, G. H. In *Antibiotic Discovery and Development*; Dougherty, T. J., Pucci, M. J., Eds.; Springer Science+Business Media: Berlin, 2012; pp 229−269.

(17) Becker, B.; Cooper, M. A. *ACS Chem. Biol.* **2013**, *8*, 105−115.

(18) Poulikakos, P.; Falagas, M. E. *Exp. Opin. Pharmacother.* **2013**, *14*, 1585−1597.

(19) Vakulenko, S. B.; Mobashery, S. *Clin. Microbiol. Rev.* **2003**, *16*, 430−450.

(20) Jackson, J.; Chen, C.; Buising, K. *Curr. Opin. Infect. Dis.* **2013**, *26*, 516−525.

(21) Fosso, M. Y.; Li, Y.; Garneau-Tsodikova, S. *Med. Chem. Commun.* **2014**, *5*, 1075−1091.

(22) *Critically Important Antimicrobials for Human Medicine: Categorization for the Development of Risk Management Strategies to contain Antimicrobial Resistance due to Non-Human Antimicrobial Use*, Report of the Second WHO Expert Meeting, Copenhagen, May 29−31, 2007; WHO: Geneva, Switzerland, 2007.

(23) Chambers, H. F. In *Goodman and Gilman's The Pharmaceutical Basis of Therapeutics*; 10th ed.; Hardman, J. G., Limbird, L. E., Eds.; McGraw-Hill: New York, 1996; pp 1103−1121.

DOI: 10.1021/jacs.5b02248
J. Am. Chem. Soc. 2015, 137, 7706−7717

(24) Hanberger, H.; Edlund, C.; Furebring, M.; Giske, C. G.; Melhus, A.; Nilsson, L. E.; Petersson, J.; Sjölin, J.; Ternhag, A.; Werner, M.; Eliasson, E. *Scand. J. Infect. Dis.* **2013**, *45*, 161−175.
(25) Carter, A. P.; Clemons, W. M.; Brodersen, D. E.; Morgan-Warren, R. J.; Wimberly, B. T.; Ramakrishnan, V. *Nature* **2000**, *407*, 340−348.
(26) Garreau de Loubresse, N.; Prokhorova, I.; Holtkamp, W.; Rodnina, M. V.; Yusupova, G.; Yusupov, M. *Nature* **2014**, *513*, 517−523.
(27) François, B.; Russell, R. J. M.; Murray, J. B.; Aboul-ela, F.; Masquid, B.; Vicens, Q.; Westhof, E. *Nucleic Acids Res.* **2005**, *33*, 5677−5690.
(28) Peske, F.; Savelsbergh, A.; Katunin, V. I.; Rodnina, M. V.; Wintermeyer, W. *J. Mol. Biol.* **2004**, *343*, 1183−1194.
(29) Feldman, M. B.; Terry, D. S.; Altman, R. B.; Blanchard, S. C. *Nat. Chem. Biol.* **2010**, *6*, 54−62.
(30) Moazed, D.; Noller, H. F. *Nature* **1987**, *327*, 389−394.
(31) Tsai, A.; Uemura, S.; Johansson, M.; Puglisi, E. V.; Marshall, R. A.; Echeverría Aitken, C.; Korlach, J.; Ehrenberg, M.; Puglisi, J. D. *Cell Rep.* **2013**, *3*, 497−508.
(32) Marshall, R. A.; Puglisi, J. D. In *Aminoglycoside Antibiotics: From Chemical Biology to Drug Discovery*; Ayra, D. P., Ed.; Wiley: Hoboken, NJ, 2007; pp 181−207.
(33) Kondo, J.; Westhof, E. In *Antibioitcs: Targets, Mechanisms and Resistance*; Gualerzi, C. O., Brandi, L., Fabbretti, A., Pon, C. L., Eds.; Wiley-VCH: Weinheim, 2014; pp 453−470.
(34) Weizman, H.; Tor, Y. In *Carbohydrate-Based Drug Discovery*; Wong, C.-H., Ed.; Wiley-VCH: Weinheim, 2003; Vol. *2*, pp 661−683.
(35) Magnet, S.; Blanchard, J. S. *Chem. Rev.* **2005**, *105*, 477−497.
(36) Houghton, J. L.; Green, K. D.; Chen, W.; Garneau-Tsodikova, S. *ChemBioChem* **2010**, *11*, 880−902.
(37) Ramirez, M. S.; Tolmasky, M. E. *Drug Resist. Updates* **2010**, *13*, 151−171.
(38) Labby, K. J.; Garneau-Tsodikova, S. *Fut. Med. Chem.* **2013**, *5*, 1285−1309.
(39) Yang, L.; Ye, X. S. *Curr. Top. Med. Chem.* **2010**, *10*, 1898−1926.
(40) Umezawa, S. *Adv. Carbohydr. Chem. Biochem.* **1974**, *30*, 111−182.
(41) Haddad, J.; Liu, M.-Z.; Mobashery, S. In *Glycochemistry: Principles, Synthesis, and Applications*; Wang, P. G., Bertozzi, C. R., Eds.; Dekker: New York, 2001; pp 353−424.
(42) Wang, J.; Chang, C.-W. T. In *Aminoglycoside Antibiotics*; Arya, D. P., Ed.; Wiley: Hoboken, NJ, 2007; pp 141−180.
(43) Berkov-Zrihen, Y.; Fridman, M. In *Modern Synthetic Methods in Carbohydrate Chemistry; From Monosaccharides to Complex Glycoconjugates*; Werz, D. B., Vidal, S., Eds.; Wiley: Weinheim, 2014; pp 161−190.
(44) Aggen, J. B.; Armstrong, E. S.; Goldblum, A. A.; Dozzo, P.; Linsell, M. S.; Gliedt, M. J.; Hildebrandt, D. J.; Feeney, L. A.; Kubo, A.; Matias, R. D.; Lopez, S.; Gomez, M.; Wlasichuk, K. B.; Diokno, R.; Miller, G. H.; Moser, H. E. *Antimicrob. Agents Chemother.* **2010**, *54*, 4636−4642.
(45) Zhanel, G. G.; Lawson, C. D.; Zelenitsky, S.; Findlay, B.; Schweizer, F.; Adam, H.; Walkty, A.; Rubinstein, E.; Gin, A. S.; Hoban, D. J.; Lynch, J. P.; Karlowsky, J. A. *Exp. Rev. Anti-infect. Ther.* **2012**, *10*, 459−473.
(46) Hanessian, S.; Maianti, J. P.; Matias, R. D.; Feeney, L. A.; Armstrong, E. S. *Org. Lett.* **2011**, *13*, 6476−6479.
(47) Maianti, J. P.; Kanazawa, H.; Dozzo, P.; Matias, R. D.; Feeney, L. A.; Armstrong, E. S.; Hildebrandt, D. J.; Kane, T. R.; Gliedt, M. J.; Goldblum; Linsell, M. S.; Aggen, J. B.; Kondo, J.; Hanessian, S. *ACS Chem. Biol.* **2014**, *9*, 2067−2073.
(48) Mingeot-Leclercq, M.-P.; Tulkens, P. M. *Antimicrob. Agents Chemother.* **1999**, *43*, 1003−1012.
(49) Avent, M. L.; Rogers, B. A.; Cheng, A. C.; Paterson, D. L. *Int. Med.* **2011**, *41*, 441−449.
(50) Duggal, P.; Sarkar, M. *BMC Ear Nose Throat Disord.* **2007**, DOI: 10.1186/1472-6815-7-5.
(51) Peloquin, C. A.; Berning, S. E.; Nitta, A. T.; Simone, P. M.; Goble, M.; Huitt, G. A.; Iseman, M. D.; Cook, J. L.; Curran-Everett, D. *Clin. Infect. Dis.* **2004**, *38*, 1538−1544.
(52) Prezant, T. R.; Agapian, J. V.; Bohlman, M. C.; Bu, X.; Öztas, S.; Qiu, W.-Q.; Arnos, K. S.; Cortopassi, G. A.; Jaber, L.; Rotter, J. I.; Shohat, M.; Fischel-Ghodsian, N. *Nat. Genet.* **1993**, *4*, 289−294.
(53) Böttger, E. C.; Schacht, J. *Hearing Res.* **2013**, *303*, 12−19.
(54) Hobbie, S. N.; Akshay, S.; Kalapala, S. K.; Bruell, C.; Shcherbakov, D.; Böttger, E. C. *Proc. Natl. Acad. Sci. U.S.A.* **2008**, *105*, 20888−20893.
(55) Hobbie, S. N.; Bruell, C. M.; Akshay, S.; Kalapala, S. K.; Shcherbakov, D.; Böttger, E. C. *Proc. Natl. Acad. Sci. U.S.A.* **2008**, *105*, 3244−3249.
(56) Hobbie, S. N.; Kalapala, S. K.; Akshay, S.; Bruell, C.; Schmidt, S.; Dabow, S.; Vasella, A.; Sander, P.; Böttger, E. C. *Nucleic Acids Res.* **2007**, *35*, 6086−6093.
(57) Francis, S. P.; Katz, J.; Fanning, K. D.; Harris, K. A.; Nicholas, B. D.; Lacy, M.; Pagana, J.; Agris, P. F.; Shin, J.-B. *J. Neurosci.* **2013**, *33*, 3079−3093.
(58) Shulman, E.; Belakhov, V.; Wei, G.; Kendall, A.; Meyron-Holtz, E. G.; Ben-Shachar, D.; Schacht, J.; Baasov, T. *J. Biol. Chem.* **2014**, *289*, 2318−2330.
(59) Henley, C. M.; Schacht, J. *Audiology* **1988**, *27*, 137−146.
(60) Dulon, D.; Aran, J. M.; Zajic, G.; Schacht, J. *Antimicrob. Agents Chemother.* **1986**, *30*, 96−100.
(61) Aran, J. M.; Chappert, C.; Dulon, D.; Erre, J. P.; Aurousseau, C. *Hearing Res.* **1995**, *82*, 179−183.
(62) Matt, T.; Ng, C. L.; Lang, K.; Sha, S.-H.; Akbergenov, R.; Shcherbakov, D.; Meyer, M.; Duscha, S.; Xie, J.; Dubbaka, S. R.; Perez-Fernandez, D.; Vasella, A.; Ramakrishnan, V.; Schacht, J.; Böttger, E. C. *Proc. Natl. Acad. Sci. U.S.A.* **2012**, *109*, 10984−10989.
(63) Meyer, M.; Freihofer, P.; Scherman, M.; Teague, J.; Lenaerts, A.; Böttger, E. C. *Antimicrob. Agents Chemother.* **2014**, *54*, 6938−6941.
(64) Perez-Fernandez, D.; Shcherbakov, D.; Matt, T.; Leong, N. C.; Kudyba, I.; Duscha, S.; Boukari, H.; Patak, R.; Dubbaka, S. R.; Lang, K.; Meyer, M.; Akbergenov, R.; Freihofer, P.; Vaddi, S.; Thommes, P.; Ramakrishnan, V.; Vasella, A.; Böttger, E. C. *Nature Commun.* **2014**, DOI: 10.1038/ncomms4112.
(65) Duscha, S.; Boukari, H.; Shcherbakov, D.; Salian, S.; Silva, S.; Kendall, A.; Kato, T.; Akbergenov, R.; Perez-Fernandez, D.; Bernet, B.; Vaddi, S.; Thommes, P.; Schacht, J.; Crich, D.; Vasella, A.; Böttger, E. C. *mBio* 5 (5): e01827-14 10.1128/mBio.01827-14.
(66) Mandhapati, A. R.; Shcherbakov, D.; Duscha, S.; Vasella, A.; Böttger, E. C.; Crich, D. *ChemMedChem* **2014**, *9*, 2074−2083.
(67) Chen, W.; Matsushita, T.; Shcherbakov, D.; Boukari, H.; Vasella, A.; Böttger, E. C.; Crich, D. *MedChemComm* **2014**, *5*, 1179−1187.
(68) Pathak, R.; Perez-Fernandez, D.; Nandurdikar, R.; Kalapala, S. K.; Böttger, E. C.; Vasella, A. *Helv. Chim. Acta* **2008**, *91*, 1533−1552.
(69) Qiu, D.; Schmidt, R. R. *Synthesis* **1990**, 875−877.
(70) Hada, N.; Miyamura, A.; Ohtsuka, I.; Kiuchi, F. *Heterocycles* **2014**, *88*, 689−704.
(71) Zhao, G.-L.; Yu, Z.-Y.; Li, Y.; Pang, L.-N.; Wang, J.-W. *Chin. J. Chem.* **2008**, *26*, 158−164.
(72) Sato, T.; Fujita, Y.; Otera, J.; Nozaki, H. *Tetrahedron Lett.* **1992**, *33*, 239−242.
(73) Kametani, T.; Kawamura, K.; Honda, T. *J. Am. Chem. Soc.* **1987**, *109*, 3010−3017.
(74) Touisni, N.; Maresca, A.; McDonald, P. C.; Lou, Y.; Scozzafava, A.; Dedhar, S.; Winum, J.-y.; Supuran, C. T. *J. Med. Chem.* **2011**, *54*, 8271−8277.
(75) Chiu-Machado, I.; Castro-Palomino, J. C.; Madrazo-Alonso, O.; Loipetegui-Palacios, C.; Verez-Bencomo, V. *J. Carbohydr. Chem.* **1995**, *14*, 551−561.
(76) Lafont, D.; Descotes, G. *Carbohydr. Res.* **1987**, *166*, 195−209.
(77) Costantino, V.; Imperatore, C.; Fattorusso, E.; Mangoni, A. *Tetrahedron Lett.* **2000**, *41*, 9177−9180.
(78) Codée, J. D. C.; van den Bos, L. J.; Litjens, R. E. J. N.; Overkleeft, H. S.; van Boeckel, C. A. A.; van Boom, J. H.; van der Marel, G. A. *Tetrahedron* **2004**, *60*, 1057−1064.

DOI: 10.1021/jacs.5b02248
J. Am. Chem. Soc. 2015, 137, 7706−7717

(79) Crich, D.; Smith, M.; Yao, Q.; Picione, J. *Synthesis* **2001**, 323−326.
(80) Konradsson, P.; Mootoo, D. R.; McDevitt, R. E.; Fraser-Reid, B. *J. Chem. Soc., Chem. Commun.* **1990**, 270−272.
(81) Konradsson, P.; Udodong, U. E.; Fraser-Reid, B. *Tetrahedron Lett.* **1990**, *31*, 4313−4316.
(82) Schmidt, R. R. *Angew. Chem., Int. Ed.* **1986**, *25*, 212−235.
(83) Issa, J. P.; Lloyd, D.; Steliotes, E.; Bennett, C. S. *Org. Lett.* **2013**, *15*, 4170−4173.
(84) Issa, J. P.; Bennett, C. S. *J. Am. Chem. Soc.* **2014**, *136*, 5740−5744.
(85) McNaught, A. D. *Carbohydr. Res.* **1997**, *297*, 1−92.
(86) Abe, Y.; Nakagawa, S.; Naito, T.; Kawaguchi, H. *J. Antibiot.* **1981**, *34*, 1434−1446.
(87) Chang, C.-W. T.; Hui, Y.; Elchert, B.; Wang, J.; Li, J.; Rai, R. *Org. Lett.* **2002**, *4*, 4603−4606.
(88) Wang, J.; Li, J.; Tuttle, D.; Takemoto, J. Y.; Chang, C.-W. T. *Org. Lett.* **2002**, *4*, 3997−4000.
(89) Fridman, M.; Belakhov, V.; Yaron, S.; Baasov, T. *Org. Lett.* **2003**, *5*, 3575−3578.
(90) Seeberger, P. H.; Baumann, M.; Zhang, G.; Kanemitsu, T.; Swayze, E. E.; Hofstadler, S. A.; Griffey, R. H. *Synlett* **2003**, 1323−1326.
(91) Elchert, B.; Li, J.; Wang, J.; Hui, Y.; Rai, R.; Ptak, R.; Ward, P.; Takemoto, J. Y.; Bensaci, M.; Chang, C.-W. T. *J. Org. Chem.* **2004**, *69*, 1513−1523.
(92) Hainrichson, M.; Pokrovskaya, V.; Shallom-Shezifi, D.; Fridman, M.; Belakhov, V.; Shachar, D.; Yaron, S.; Baasov, T. *Bioorg. Med. Chem.* **2005**, *13*, 5797−5807.
(93) Wang, J.; Li, J.; Chen, H.-N.; Chang, H.; Tanifum, C. T.; Liu; Czyryca, P. G.; Chang, C.-W. T. *J. Med. Chem.* **2005**, *48*, 6271−6285.
(94) Revuelta, J.; Vacas, T.; Bastida, A.; Asensio, J. L. *Chem.—Eur. J.* **2010**, *16*, 2986−2991.
(95) Rao, V. S. R.; Qasba, P. K.; Balaji, P. V.; Chandrasekaran, R. *Conformation of Carbohydrates*; Harwood Academic Publishers: Amsterdam, 1998.
(96) Grindley, T. B. In *Glycoscience: Chemistry and Chemical Biology*; Fraser-Reid, B., Tatsuta, K., Thiem, J., Eds.; Springer: Berlin, 2001; Vol. *1*, pp 3−51.
(97) Duus, J. O.; Gotfredsen, C. H.; Bock, K. *Chem. Rev.* **2000**, *100*, 4589−4614.
(98) Altona, C.; Sundaralingam, M. *J. Am. Chem. Soc.* **1972**, *94*, 8205−8212.
(99) Costantino, V.; Fattorusso, E.; Imperatore, C.; Mangoni, A. *J. Org. Chem.* **2008**, *73*, 6158−6165.
(100) Taha, H. A.; Castillo, N.; Sears, D. N.; Wasylishen, R. E.; Lowary, T. L.; Roy, P.-N. *J. Chem. Theory Comput.* **2010**, *6*, 212−222.
(101) Taha, H. A.; Roy, P.-N.; Lowary, T. L. *J. Chem. Theory Comput.* **2011**, *7*, 420−432.
(102) Houseknecht, J. B.; Lowary, T. L.; Hadad, C. M. *J. Phys. Chem. A* **2003**, *107*, 5763−5777.
(103) Taha, H. A.; Richards, M. R.; Lowary, T. L. *Chem. Rev.* **2013**, *113*, 1851−1876.
(104) Nahoum, V.; Spector, S.; Loll, P. *Acta Crystallogr., Sect. D* **2011**, *67*, 592.
(105) Chu, S. S. C.; Jeffrey, G. A. *Acta Crystallogr., Sect. B* **1968**, *24*, 830−838.
(106) Brown, C. J. *J. Chem. Soc. A* **1966**, 927−932.
(107) Jacobson, R. A.; Wunderlich, J. A.; Lipscomb, W. N. *Acta Crystallogr., Sect. B* **1961**, *24*, 598−607.
(108) Ham, J. T.; Williams, D. G. *Acta Crystallogr., Sect. B* **1970**, *26*, 1373−1383.
(109) Bernet, B.; Vasella, A. *Helv. Chim. Acta* **2000**, *83*, 2055−2071.
(110) Bohner, T. V.; Verena, B.; Vasella, A. *Helv. Chim. Acta* **1999**, *82*, 198−228.
(111) Ogle, J. M.; Ramakrishnan, V. *Annu. Rev. Biochem.* **2005**, *74*, 129−177.
(112) Akbergenov, R.; Shcherbakov, D.; Matt, T.; Duscha, S.; Meyer, M.; Perez-Fernandez, D.; Pathak, R.; Harish, S.; Kudyba, I.; Dubbaka, S. R.; Silva, S.; Ruiz Ruiz, M.; Salian, S.; Vasella, A.; Böttger, E. C. In *Ribosomes: Structure, Function, and Dynamics*; Rodnina, M. V., Wintermeyer, W., Green, R., Eds.; Springer-Verlag: Vienna, 2011; pp 249−261.
(113) Pfister, P.; Hobbie, S.; Vicens, Q.; Böttger, E. C.; Westhof, E. *ChemBioChem* **2003**, *4*, 1078−1088.
(114) Greber, B. J.; Bieri, P.; Leibundgut, M.; Leitner, A.; Aebersold, R.; Boehringer, D.; Ban, N. *Science* **2015**, *348*, 303−308.
(115) Amunts, A.; Brown, A. D.; Toots, J.; Scheres, S. H. W.; Ramakrishnan, V. *Science* **2015**, *348*, 95−98.
(116) Ida, T.; Okamoto, R.; Shimauchi, C.; Okubo, T.; Kuga, A.; Inoue, M. *J. Clin. Microbiol.* **2001**, *39*, 3115−3121.
(117) Yan, R.-B.; Yuan, M.; Wu, Y.; You, X.; Ye, X.-S. *Bioorg. Med. Chem.* **2011**, *19*, 30−40.

DOI: 10.1021/jacs.5b02248
J. Am. Chem. Soc. 2015, 137, 7706−7717